The Astrojax Pendulum and the N-Body Problem on the Sphere: A study in reduction, variational integration, and pattern evocation.

Philip Du Toit

1 June 2005

Abstract

We study the Astrojax Pendulum and the N-body problem on the sphere in the light of Lagrangian reduction theory, variational integrators, and pattern evocation.

1 Introduction

The main intent of this research is to use a simple mechanical example to explore the topics of variational integration, pattern evocation, and reduction theory. This paper serves as preliminary work for future research into how structure and symmetry of manifolds influence mechanical systems. In the first three sections, foundation principles in Lagrangian reduction, variational integrators, and pattern evocation are established. In the later sections, we apply these principles to the mechanical examples of the Astrojax pendulum and the N-body problem on the sphere.

2 Lagrangian Reduction

In this section, we outline the method of Lagrangian reduction generally. The discussion follows the exposition given in [Marsden, Ratiu] and [Bloch]. Later, we will apply the method presented here to the specific case of the Astrojax Pendulum. An exactly similar and more well-known reduction can be performed on the Hamiltonian side using Poisson structures and symplectic reduction, but this approach is not presented here.

Let Q be a configuration manifold. Let G be a lie group with lie algebra $\mathfrak{g}$. Suppose that G acts freely and properly on Q and that the metric $\langle\langle\ ,\ \rangle\rangle$ is invariant under the action of G. Let G act on TQ by a lift of the tangent

mapping. Let the Lagrangian $L : TQ \to \mathbb{R}$, be a G-invariant Lagrangian. Then we define the momentum map $\mathbf{J} : TQ \to \mathfrak{g}^*$ by

$$\langle \mathbf{J}(v_q), \xi \rangle = \langle \mathbb{F}L(v_q), \xi_Q(q) \rangle$$

where $v_q \in TQ$, $\xi \in \mathfrak{g}$, and $\mathbb{F}L(v_q)$ is the fiber derivative of L in the fiber direction. Then, in this context, we have the celebrated Theorem of Noether:

Theorem 2.1 (Noether's Theorem)
If L is a G-invariant Lagrangian on TQ, then for a solution of the Euler-Lagrange equations, $\mathbf{J}$ is conserved.

Before proceeding to obtain the reduced Lagrangian on TQ/G, we need to first introduce the infinitesimal generator of the group action as well as two more mappings: the locked inertia tensor and the mechanical connection.

Recall that the *infinitesimal generator* of the action of G on Q corresponding to $\xi \in \mathfrak{g}$ is a vector field on Q defined by

$$\xi_Q(q) = \left. \frac{d}{dt} \right|_{t=0} e^{t\xi}(q) \, .$$

For each $q \in Q$, we define the *locked inertia tensor* to be the map $\mathbb{I} : \mathfrak{g} \to \mathfrak{g}^*$ defined by

$$\langle \mathbb{I}\eta, \zeta \rangle = \langle\langle \eta_Q(q) \, , \, \zeta_Q(q) \rangle\rangle \, .$$

We define the *mechanical connection* on the principal bundle $Q \to Q/G$ to be the map $\mathcal{A} : TQ \to \mathfrak{g}$ given by

$$\mathcal{A}(q, v) = \mathbb{I}(q)^{-1}\big(\mathbf{J}(q, v)\big) \, .$$

Heuristically, we can think of the locked inertia tensor as assigning to each element of the configuration space an inertia tensor corresponding to the action of G on Q. For example, the locked inertia tensor corresponding to the action of rotation by the group S^1 assigns to each $q \in Q$ the moment of inertia about the axis of rotation as though the configuration were locked or "welded" fixed. Then, for a fixed value of the momentum map $\mathbf{J}$, the mechanical connection $\mathcal{A}$ assigns to each $(q, v) \in TQ$ the corresponding angular velocity of the locked system.

Next we define the reduced Lagrangian for mechanical systems as given in [Bloch] section 3.11. Let $L : TQ \to \mathbb{R}$ be a G-invariant Lagrangian. The *reduced Lagrangian* $l : TQ/G \to \mathbb{R}$ is defined as

$$l(r, \xi, \dot{r}) = L(r, g^{-1}g, \dot{r}, g^{-1}\dot{g})$$

where $\xi = (g^{-1}\dot{g}, r, \dot{r})$ are local coordinates on TQ/G. In more familiar terms, we say that the ξ are the body velocities with respect to the body frame, and $\xi^s = \dot{g}g^{-1}$ are the spatial velocities. Then, for a mechanical system with Lagrangian of the form

$$L(q, v_q) = \frac{1}{2} \langle\langle v_q, v_q \rangle\rangle - V(q)$$

we have the following result proved in [Bloch]:

Theorem 2.2 (*Reduced Lagrangian)*
For a G-invariant mechanical Lagrangian the reduced Lagrangian may be written in the form

$$l(r,\dot{r},\xi) = \frac{1}{2}(\xi^T, \dot{r}^T)\begin{bmatrix} I & IA \\ A^T I & m(r) \end{bmatrix}\begin{bmatrix} \xi \\ \dot{r} \end{bmatrix} - V(r)$$

where I is the local form of the locked inertia tensor and A is the local form of the mechanical connection.

3 Variational Integrators

Traditional numerical integration techniques begin with a discretization scheme at the level of the equations of motion. In this section, we present the idea of constructing discrete algorithms for approximating trajectories of a mechanical system by discretizing the original variational principle from which the equations of motion are derived. Employing a discrete variational principle is attractive since the resulting algorithm respects the invariants of the original continuous system and preserves the symplectic form.

First, we must state precisely what is meant by a discrete variational principle. The derivation given here follows that given by [Wendlandt, Marsden; 1997]. Let $L : TQ \to \mathbb{R}$ be a Lagrangian for a mechanical system. In the continuous setting, the variational principle of Hamilton states that the solution trajectory through Q is the curve $q(t)$ such that the

$$\delta \int_a^b L(q^i, \dot{q}^i, t)\, dt = 0\,.$$

Variations of the action integral are taken over all curves in Q with the end points held fixed. It is a standard exercise to show that this principle is equivalent to the statement that $q(t)$ satisfies the Euler-Lagrange equations:

$$\frac{d}{dt}\frac{\partial L}{\partial \dot{q}^i} - \frac{\partial L}{\partial q^i} = 0\,, \qquad i = 1, \cdots, n.$$

Now we place Hamilton's principle in a discrete setting. Given the continuous Lagrangian $L : TQ \to \mathbb{R}$, we introduce the discrete Lagrangian $L_d : Q \times Q \to \mathbb{R}$. The order to which L_d approximates L determines the order of accuracy of the method. For example, for $x, y \in Q$ we may choose

$$L_d(x,y) = L\left(\frac{x+y}{2}, \frac{y-x}{h}\right)$$

where $h \in \mathbb{R}^+$ is the time step of the method and $\left(\frac{x+y}{2}, \frac{y-x}{h}\right)$ is a first order approximation to $v_q \in TQ$. In analogy to the action integral, we define the action sum $\mathbb{S} : Q^{N+1} \to \mathbb{R}$ by

$$\mathbb{S} = \sum_{k=0}^{N-1} \mathrm{L}_d(q_k, q_k + 1)$$

where $q_k \in Q$ and $k \in \mathbb{Z}$ is the discrete time. The discrete Hamilton's principle states that the trajectory of the system extremizes the action sum. That is, the trajectory q^k, $k = 1 \cdots N$, satisfies

$$\delta \sum_{k=0}^{N-1} \mathrm{L}_d(q_k, q_k + 1) = 0$$

where variations are taken over points in Q with the end points held fixed. Again, it is straight forward to show that this discrete principle is equivalent to the implicit time-stepping algorithm defined by

$$D_1 L_d(q_k + q_{k+1}) + D_2 L(q_{k-1}, q_k) = 0 \qquad \text{for all } k \in \{1, \cdots, N-1\}.$$

This set of equations is called the *Discrete Euler-Lagrange Equations*. The equations implicitly define a map $(q_{k-1}, q_k) \to (q_k, q_{k+1})$ which is the time-stepping algorithm. We call an algorithm derived in this way a variational integrator.

In [Wendlandt, Marsden; 1997] it is shown that variational integrators preserve both the symplectic form and the momentum map. Furthermore, a discrete version of Noether's theorem is derived and it is noted that a discrete version of reduction theory may be applied in the discrete case.

4 Pattern Evocation

We have presented previously the concept of reduction. From
[Marsden, Scheurle, Wendlandt; 1995], we have the result that if the reduced system exhibits a periodic orbit, then when viewed in a suitably chosen rotating frame with constant angular velocity, the orbit in the original unreduced space is also periodic. We now elaborate on this result using the notation we have introduced thus far.

Let Q be a manifold. Let G be a lie group that acts freely and properly on Q. Let $\pi : Q \to Q/G =: S$ be a principal G-bundle that projects from the configuration manifold Q to the shape space (the reduced space) S. Let L be a $G-$invariant Lagrangian on Q. Let $\mathbf{J} : T^*Q \to \mathfrak{g}^*$ be the standard equivariant cotangent bundle momentum map for the cotangent lifted action of G on T^*Q. Choose a momentum value $\mu \in \mathfrak{g}^*$. Let the locked inertia tensor be the map $\mathbb{I}(q) : \mathfrak{g} \to \mathfrak{g}^*$. Define the map $\alpha : TQ \to \mathfrak{g}$ which assigns the angular velocity of the locked system:

$$\alpha(q, v) = \mathbb{I}(q)^{-1} J(q, v).$$

The map α is a mechanical connection on the principal bundle. Also, use α to define α_μ, a one-form on Q by

$$\langle \alpha_\mu(q), v_q \rangle = \langle \mu, \alpha(v_q) \rangle \ .$$

Define the ammended potential $V_\mu := V(q) + \frac{1}{2}\langle \mu, \mathbb{I}_q^{-1}\mu \rangle$. Suppose that $z_e \in T^*_{q_e}$ lies on $\mathbf{J}^{-1}(\mu)$. Then, z_e is a relative equilibrium if and only if q_e is a critical point of V_μ, and z_e is of the form $\alpha_\mu(q_e)$.

A specific example may help to elucidate the notation. Consider a simple spherical pendulum. The Lagrangian is invariant under the action of S^1 about the z-axis. An equilibrium point in the reduced shape space corresponds to a fixed shape which is rotated steadily about the z-axis under the action of the group. In the reduced space, the potential is ammended to include not only the gravitational potential but also the effective potential of the non-inertial forces in the unreduced space. Therefore, the equilibrium point z_e in shape space corresponds to a critical point of the ammended potential. Precisely in this sense, the so-called conical pendulum is an example of a relative equilibrium. The motion of the conical pendulum is entirely described by

$$z(t) = e^{t\xi} z_e$$

for some $\xi \in \mathfrak{g}$, the Lie algebra of G.

With these ideas now in place, we can state the pattern evocation theorem from [Marsden, Scheurle, Wendlandt; 1995] explicitly:

Theorem 4.1 (Pattern Evocation)
Assume that the exponential map $\exp : \mathfrak{g} \to G$ *is surjective. Assume that* $c(t)$ *is a relative periodic orbit and denote a period of the reduced orbit by* T*. Then there is a Lie algebra element* $\gamma \in \mathfrak{g}$ *such that* $\exp(-\gamma t)c(t)$ *is also periodic with period* T*.*

5 The Astrojax Pendulum

An interesting toy problem is the Astrojax pendulum. The physical set up of the Astrojax is essentially a double spherical pendulum in which the first bob is allowed to slide freely on the tether. Players of the Astrojax can produce many exciting and unexpected motions. Indeed, even without external forcing from a player, the motion of the two bobs exhibits intricate and chaotic behavior. More information about the Astrojax and movies of players performing tricks with the Astrojax can be viewed online at www.astrojax.com

5.1 Mathematical Model

We model the Astrojax with a massless tether of fixed length l and two constrained point masses, m_1 and m_2, moving in a gravitational field. Figure 1 is a schematic illustration of the Astrojax pendulum. One end of the tether is attached to a rigid support. The first mass, m_1, is constrained implicitly by the requirement that if m_1 is a distance λ from the pivot, then m_2 must be a distance $l - \lambda$ from m_2. Thus, in contrast to the double spherical pendulum, this system has only one constraint. Namely, the sum of the straight line distances between the pivot and m_1, and m_1 and m_2 (the tether length) remain constant.

The position of m_1 on the tether defines a vertex at which the tether can be bent. In this sense the tether is flexible. However, the two segments of the tether defined by the vertex at m_1 are treated as massless rigid rods. This

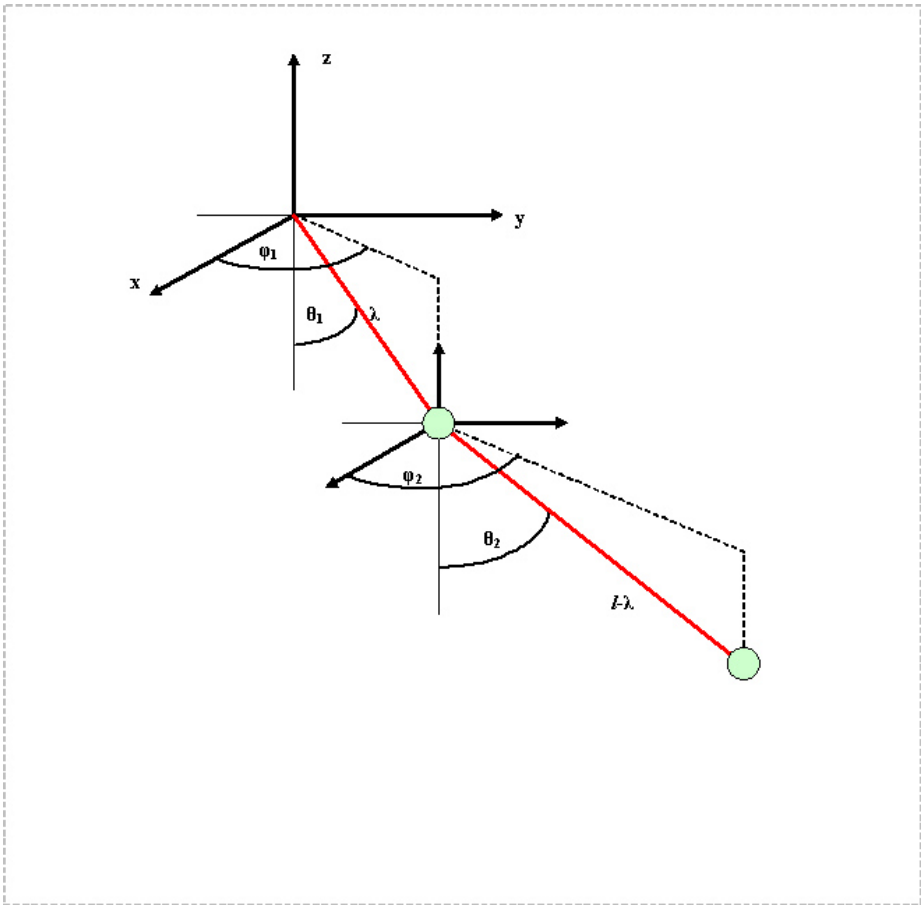

Figure 1: The Astrojax Pendulum

agrees with movies of real Astrojax players in which the tether segments always remain taught.

The Astrojax exhibits 5 degrees of freedom. The configuration space is $Q = S^2 \times S^2 \times \mathbb{R}$. The distance from the support to m_1 is $\lambda \in \mathbb{R}$. Then, the positions of m_1 and m_2 are uniquely specified by the spherical coordinates (θ_1, ϕ_1) and (θ_2, ϕ_2) respectively.

A simplification of the Astrojax is to consider only motion in a vertical plane. In this case, the system has three degrees of freedom. The configuration space is $Q = S^1 \times S^1 \times \mathbb{R}$ with coordinates $(\lambda, \theta_1, \theta_2)$.

It is important to realize at this point what is *not* specified by this model. In particular, the constraint does not require that m_1 remain between the support and m_2. Indeed, the distance from the pivot to m_1, λ, is not restricted to be in $[0, l]$. More to the point, the distance between m_1 and m_2, $l - \lambda$, need not be positive! If we prefer to only consider distances as positive quantities, then a better interpretation is that if $\lambda > l$, then the direction of gravity for m_2 is reversed. In summary, no additional constraints involving inequalities or absolute values were used to make sure that m_1 bounces off m_2 instead of flying off the tether. Moreover, this model has nothing to say about collisions between the the two masses or the first mass and the support. The masses are free to slide through each other. Nevertheless, it is remarkable how well this model, despite its simplicity, is able to capture the dynamics of the collisions and knows to keep m_1 between the support and m_2. This behavior will be seen in the simulations, but the reader should be aware that these collision dynamics were not explicitly incorporated into the equations.

A few sample simulations for the planar Astrojax pendulumare provided below. The simulations were produced using an implicit differential equation solver with adaptive time-stepping in Matlab

1. Initial condition: $\theta_1 = \frac{\pi}{4}$ and $\theta_2 = \frac{\pi}{4}$. This simulation displays typical motion of the Astrojax pendulumand demonstrates how the model incorporates collisions. Watch Movie

2. Initial condition: $\theta_1 = \frac{3\pi}{4}$ and $\theta_2 = \frac{3\pi}{4}$. This simulation demonstrates more energetic motion above the height of the pivot. Watch Movie

3. Initial condition: $\theta_1 = \frac{\pi}{4}$ and $\theta_2 = \frac{\pi}{4}$ but with $m_1 = 10m_2$. The whiplash effect is accentuated in this movie because of the disparity in the masses. Watch Movie

4. Initial condition: $\theta_1 = 0.05$ and $\theta_2 = 0$. This simulation demonstrates the ability of the model to reproduce bouncing motion and collisions. Watch Movie

5.2 Euler-Lagrange Equations

We initiate an analysis of the Astrojax pendulum by deriving the Lagrangian, $L = T - V$. The potential energy term, V, is straightforward:

$$V = -m_1 g \lambda \cos\theta_1 + m_2 g(\lambda \cos\theta_1 + (l-\lambda)\cos\theta_2\,.$$

In order to determine the kinetic energy term,

$$K = \frac{1}{2} m_1 (\dot{\mathbf{q}}_1 \cdot \dot{\mathbf{q}}_1) + \frac{1}{2} m_2 (\dot{\mathbf{q}}_2 \cdot \dot{\mathbf{q}}_2)\,.$$

We first write the position vectors, $\mathbf{q}_1$ and $\mathbf{q}_2$, of both masses in terms of the generalized coordinates. Then we differentiate these position vectors with respect to time to obtain $\dot{\mathbf{q}}_1$ and $\dot{\mathbf{q}}_2$ from which K follows.

The Lagrangian for the three-dimensional Astrojax pendulum is given by

$$\begin{aligned}
L \;=\; & \frac{1}{2} m_1 \left(\dot{\lambda}^2 + \lambda^2 \dot{\theta}_1^2 + \lambda^2 \dot{\phi}_1^2 \sin^2\theta_1 \right) \\
& + \frac{1}{2} m_2 \left(\dot{\lambda}^2 + \lambda^2 \dot{\theta}_1^2 + \lambda^2 \dot{\phi}_1^2 \sin^2\theta_1 \right) \\
& + \frac{1}{2} m_2 \left(\dot{\lambda}^2 + (l-\lambda)^2 \dot{\theta}_2^2 + (l-\lambda)^2 \dot{\phi}_2^2 \sin^2\theta_2 \right) \\
& + m_2 \Bigg(-\dot{\lambda}^2 \Big[\cos\theta_1 \cos\theta_2 + \sin\theta_1 \sin\theta_2 \cos(\phi_1 - \phi_2) \Big] \\
& \qquad + \lambda \dot{\lambda} \dot{\theta}_1 \Big[\sin\theta_1 \cos\theta_2 - \cos\theta_1 \sin\theta_2 \cos(\phi_1 - \phi_2) \Big] \\
& \qquad + (l-\lambda) \dot{\lambda} \dot{\theta}_2 \Big[\sin\theta_1 \cos\theta_2 \cos(\phi_1 - \phi_2) - \cos\theta_1 \sin\theta_2 \Big] \\
& \qquad + \lambda (l-\lambda) \dot{\theta}_1 \dot{\theta}_2 \Big[\cos\theta_1 \cos\theta_2 \cos(\phi_1 - \phi_2) + \sin\theta_1 \sin\theta_2 \Big] \\
& \qquad + \dot{\lambda} \left(\lambda \dot{\phi}_1 + (l-\lambda) \dot{\phi}_2 \right) \sin\theta_1 \sin\theta_2 \sin(\phi_1 - \phi_2) \\
& \qquad + \lambda (l-\lambda) \dot{\theta}_1 \dot{\phi}_2 \cos\theta_1 \sin\theta_2 \sin(\phi_1 - \phi_2) \\
& \qquad - \lambda (l-\lambda) \dot{\phi}_1 \dot{\theta}_2 \sin\theta_1 \cos\theta_2 \sin(\phi_1 - \phi_2) \\
& \qquad + \lambda (l-\lambda) \dot{\phi}_1 \dot{\phi}_2 \sin\theta_1 \sin\theta_2 \cos(\phi_1 - \phi_2) \Bigg) \\
& + m_1 g \lambda \cos\theta_1 \\
& + m_2 g \lambda \cos\theta_1 + m_2 g (l-\lambda) \cos\theta_2\,.
\end{aligned}$$

From this point, it is a straightforward though lengthy exercise to calculate the Euler-Lagrange equations. The five Euler-Lagrange equations are provided in Appendix A.

5.3 Lagrangian Reduction on the Astrojax Pendulum

Here, we pause to observe an elementary Lagrangian reduction of the Astrojax pendulum. We begin by noticing that both the metric on Q and the potential energy function $V(q)$ are invariant under the action of S^1 about the gravity vector. Hence, the Lagrangian is invariant under rotations about the z-axis. In particular, notice that the Lagrangian depends on ϕ_1 and ϕ_2 only in the combination $\phi_1 - \phi_2$. The Lagrangian depends only on the relative angular displacement of the two bobs and not their absolute displacement. This motivates the following invertible change of variables

$$\begin{aligned} \alpha &:= \phi_1 + \phi_2 \\ \beta &:= \phi_1 - \phi_2 \end{aligned}$$

so that

$$\phi_1 = \frac{\alpha + \beta}{2}$$

$$\phi_2 = \frac{\alpha - \beta}{2}.$$

Under this change of variables the Lagrangian becomes

$$
\begin{aligned}
L(\lambda,\theta_1,\theta_2,\alpha,\beta,\dot\lambda,\dot\theta_1,\dot\theta_2,\dot\alpha,\dot\beta) \quad = \quad & \frac{1}{2}m_1\left(\dot\lambda^2+\lambda^2\dot\theta_1^2+\lambda^2\left(\frac{\dot\alpha+\dot\beta}{2}\right)^2\sin^2\theta_1\right)\\
& +\frac{1}{2}m_2\left(\dot\lambda^2+\lambda^2\dot\theta_1^2+\lambda^2\left(\frac{\dot\alpha+\dot\beta}{2}\right)^2\sin^2\theta_1\right)\\
& +\frac{1}{2}m_2\left(\dot\lambda^2+(l-\lambda)^2\dot\theta_2^2+(l-\lambda)^2\left(\frac{\dot\alpha-\dot\beta}{2}\right)^2\sin^2\theta_2\right)\\
& +m_2\Bigg(-\dot\lambda^2\Big[\cos\theta_1\cos\theta_2+\sin\theta_1\sin\theta_2\cos\beta\Big]\\
& \qquad +\lambda\dot\lambda\dot\theta_1\Big[\sin\theta_1\cos\theta_2-\cos\theta_1\sin\theta_2\cos\beta\Big]\\
& \qquad +(l-\lambda)\dot\lambda\dot\theta_2\Big[\sin\theta_1\cos\theta_2\cos\beta-\cos\theta_1\sin\theta_2\Big]\\
& \qquad +\lambda(l-\lambda)\dot\theta_1\dot\theta_2\Big[\cos\theta_1\cos\theta_2\cos\beta+\sin\theta_1\sin\theta_2\Big]\\
& \qquad +\dot\lambda\left(\lambda\left(\frac{\dot\alpha+\dot\beta}{2}\right)+(l-\lambda)\left(\frac{\dot\alpha-\dot\beta}{2}\right)\right)\sin\theta_1\sin\theta_2\sin\beta\\
& \qquad +\lambda(l-\lambda)\dot\theta_1\left(\frac{\dot\alpha-\dot\beta}{2}\right)\cos\theta_1\sin\theta_2\sin\beta\\
& \qquad -\lambda(l-\lambda)\left(\frac{\dot\alpha+\dot\beta}{2}\right)\dot\theta_2\sin\theta_1\cos\theta_2\sin\beta\\
& \qquad +\lambda(l-\lambda)\left(\frac{\dot\alpha+\dot\beta}{2}\right)\left(\frac{\dot\alpha-\dot\beta}{2}\right)\sin\theta_1\sin\theta_2\cos\beta\Bigg)\\
& +m_1g\lambda\cos\theta_1\\
& +m_2g\lambda\cos\theta_1+m_2g(l-\lambda)\cos\theta_2\,.
\end{aligned}
$$

Notice that in these new coordinates α is a cyclic variable. The Euler-Lagrange equation in α immediately yields a conservation law corresponding to the S^1 symmetry. The invariant momentum map is given by

$$\mathbf{J}(\mathbf{v_q}) = \frac{\partial L}{\partial\dot\alpha}\,.$$

We can develop this result in terms of the notation and theory given earlier in section 2.

We have seen that $L : TQ \to \mathbb{R}$ is a S^1-invariant Lagrangian. The lie algebra of S^1 is just $\mathbb{R}$. The infinitesimal generator for the action of the group on Q is

given by

$$\xi_Q = \frac{d}{dt}\Big|_{t=0} e^{t\xi}.z = \frac{d}{dt}\Big|_{t=0} \begin{bmatrix} \lambda \\ \theta_1 \\ \theta_2 \\ \phi_1 + t\xi + \phi_2 + t\xi \\ \phi_1 + t\xi - \phi_2 - t\xi \end{bmatrix} = \begin{bmatrix} 0 \\ 0 \\ 0 \\ 2\xi \\ 0 \end{bmatrix}$$

Recalling the definition of the momentum map, we see that

$$\begin{aligned} \langle \mathbf{J}(v_q), \xi \rangle &= \langle \mathbb{F}L(v_q), \xi_Q(q) \rangle \\ \xi \mathbf{J}(v_q) &= \begin{bmatrix} \frac{\partial L}{\partial \dot{\lambda}} & \frac{\partial L}{\partial \dot{\theta}_1} & \frac{\partial L}{\partial \dot{\theta}_2} & \frac{\partial L}{\partial \dot{\alpha}} & \frac{\partial L}{\partial \dot{\beta}} \end{bmatrix} \begin{bmatrix} 0 \\ 0 \\ 0 \\ 2\xi \\ 0 \end{bmatrix} \\ \mathbf{J}(v_q) &= 2\frac{\partial L}{\partial \dot{\alpha}}. \end{aligned}$$

The presence of the cyclic coordinate has effectively reduced the Lagrangian. By restricting to a level set of $\mathbf{J}$, we may consider the Lagrangian as a function on $(\lambda, \theta_1, \theta_2, \beta)$ only, and compute the Euler-Lagrange equations in these reduced coordinates.

We have seen how the invariance of the Lagrangian under the action of the group leads to reduction of the Lagrangian. We now proceed to the simulation of the Astrojax pendulum using a variational integrator.

5.4 Simulation using a variational integrator

The procedure for constructing a variational integrator presented here is based on the method described in [Wendlandt, Marsden; 1997]. We use the constrained Lagrangian approach.

First, we consider the system of two unconstrained particles moving in a uniform gravitational field. The configuration manifold is $U = \mathbb{R}^3 \times \mathbb{R}^3$ with $\dim U = 6$. Coordinates on U are denoted by $[x_1\, y_1\, z_1\, x_2\, y_2\, z_2]$ where (x_1, y_1, z_1) is the position of m_1 and (x_2, y_2, z_2) is the position of m_2. The unconstrained Lagrangian $L : TU \to \mathbb{R}$ is the elementary Lagrangian of two free particles moving in a gravitational field:

$$L = \frac{1}{2}\dot{q}M\dot{q} - V(q)$$

where $M = \mathrm{diag}(m_1, m_1, m_1, m_2, m_2, m_2)$ is the mass matrix and

$$V(q) = g(m_1 z_1 + m_2 z_2)$$

is the potential energy.

Next, we introduce the constraints imposed by the tether. The constrained configuration manifold is $Q = \mathbb{R} \times S^2 \times S^2$ so that $Q \subset U$. The constrained Lagrangian, L_c is defined as the restriction of L to the tangent bundle of Q:

$$L\Big|_{TQ} =: L_c : TQ \to \mathbb{R}\,.$$

The constraint is written as

$$g : U \to \mathbb{R} \qquad \text{such that} \qquad g^{-1}(0) = Q$$

where 0 is regular value of G. The constraint for the Astrojax pendulum is simply that the length of the tether must remain constant. Explicitly, we write this as

$$g(q) = \sqrt{x_1^2 + y_1^2 + z_1^2} + \sqrt{(x_2 - x_1)^2 + (y_2 - y_1)^2 + (z_2 - z_1)^2} = 0\,.$$

We enforce the constraint using a Lagrange multiplier $\mu \in \mathbb{R}$. The (seven) Discrete Euler-Lagrange equations are

$$\begin{aligned} M\left(\frac{v_{k+1} - 2v_k + v_{k-1}}{h^2}\right) + \frac{1}{2}\left(\frac{\partial V}{\partial q}\left(\frac{v_{k+1} + v_k}{2}\right) \;+\; \frac{\partial V}{\partial q}\left(\frac{v_k + v_{k-1}}{2}\right)\right) \\ -D^T g(v_k)\alpha &= 0 \\ g(v_{k+1}) &= 0\,. \end{aligned}$$

This time-stepping algorithm for numerical integration of the motion of the astrojax pendulum has been implemented in Matlab. The algorithm requires the use of the Newton-Raphson method on a seven dimensional system (6 coordinates and one lagrange multiplier) at each time step to solve for the updated configuration variables and the Lagrange multiplier μ. The exact calculations involved are included in Appendix B. Several simulations for various initial conditions follow.

1. Low Angular Momentum: This simulation is for a low value of μ, the angular momentum about the z-axis. The motion appears chaotic. Watch Movie.

2. High Angular Momentum: This simulation is for a high value of μ, the angular momentum about the z-axis. The motion appears more regular. Watch Movie

3. Intermediate Angular Momentum: This simulation is for an intermediate value of μ, the angular momentum about the z-axis. Watch Movie

Figure 2(a) shows the value of momentum at each time step during the intermediate angular momentum simulation listed above. Clearly, the algorithm preserves the invariant momentum to machine precision as guaranteed by the

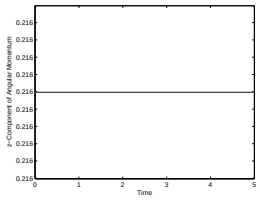

(a) zComponent of the angular momentum as a function of time.

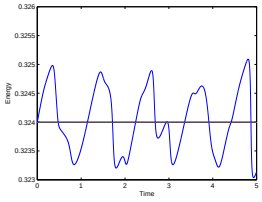

(b) Energy as a function of time.

Figure 2: Energy and Momentum Analysis of the Variational Integrator for the Astrojax Pendulum.

theory in Section 3. The theory admits no statement of energy preservation of the variational integrator algorithm; however, we see in Figure 2(b) that the energy value oscillates about its initial value with only a small relative error with even a modest choice of time step h. This property of the energy is typical of variational integrators. Indeed, it is a hallmark of variational integrators that the energy value oscillates about the true value in contrast to traditional Runga-Kutta type methods which generally exhibit decay in the energy value. In the literature, the percentage error in the energy value provides a convenient check on the validity of the simulation.

To provide further corroboration of the results obtained by the variational integrator, we simulate a known relative equilibrium solution of the double spherical pendulum. The solution is the "stretched out" relative equilibrium with initial conditions provided in [Jalnapurkar, Marsden; 1998]. The results of the simulation can be viewed in movie format. Watch Movie

5.4.1 The controlled Astrojax Pendulum

We mention here that a variational integrator for the controlled Astrojax pendulum has been developed. In an attempt to mimic actual Astrojax players, we model the control as a constraint on the position of the support. The implementation of the variational integrator for the controlled Astrojax pendulum is summarized in Appendix C.

The theory for optimal control or stabilization of relative equilibrium in the Astrojax pendulum is not presented here, but will be the topic of a future paper that will build upon the theory of control of the double spherical pendulum presented in [Jalnapurkar, Marsden; 1998]. Observation of the tricks performed by Astrojax players indicates that both the "cowboy" and the "stretched out" relative equilibrium exist in the controlled Astrojax. Of interest is the role of forcing and dissipation in the stabilization (or destabilization) of relative equilibria in the controlled Astrojax pendulum.

5.5 Pattern Evocation in the Astrojax Pendulum

We now perform an empirical search for pattern evocation in the Astrojax pendulum as outlined in [Marsden, Scheurle, Wendlandt; 1995]. For this study, we choose the trajectory given in the High Angular Momentum simulation in Section 5.4 as a test trajectory. The program in this search involves viewing the complete trajectory from a frame rotating about the z-axis for a range of rotation frequencies. Practically, we implement the search by plotting the trajectory in the following transformed coordinates:

$$\begin{bmatrix} \tilde{q}_1(t) \\ \tilde{q}_2(t) \end{bmatrix} = e^{-\hat{\xi}t} \begin{bmatrix} q_1(t) \\ q_2(t) \end{bmatrix}$$

where

$$\hat{\xi} = \begin{bmatrix} 0 & -\xi & 0 \\ \xi & 0 & 0 \\ 0 & 0 & 0 \end{bmatrix}$$

for a range of ξ values.

As the scan through the rotation frequencies proceeds, several "resonant frequencies" become evident at which simple patterns and their harmonics emerge from the apparently chaotic trajectory. A full movie depicting an animated scan through the rotation frequencies is provided here. Watch Movie. The rotation frequency at which the trajectory, extended both forward and backward in time, does not encircle the z-axis is termed the *critical frequency*. We can think of the critical frequency as the group frequency, or the frequency with which both bobs as a group rotate about the z-axis. This frequency is clearly evident in the movie scan. Notice that the resonant frequencies are characteristically different from the critical frequency which highlights the subtlety that pattern evocation is not merely an artifact of moving to a rotating frame with angular frequency equal to that of the group.

6 The N-body Problem on the Sphere

We move now to a different problem in which we can investigate further the role of symmetry and curved manifolds in mechanics. We propose studying the restriction of the N-body problem to the sphere. The N-body problem is a celebrated problem with prodigious history. Indeed, much of modern-day dynamical systems theory finds its roots in this problem. The 2-body problem on the sphere was investigated in a recent paper by Borisov, Mamaev, and Kilin.

Classically, the N-body problem refers to the mechanical system describing the motion of N point masses moving under mutual gravitational attraction according to Newton's law of gravity. Recall that Newton's law of gravity states that the force between two masses is inversely proportional to the square of the distances between them. For the present study, we propose a slightly different, but more general, problem. Consider N charged particles moving under their mutual electrostatic attraction or repulsion. This system also exhibits a force law that is inversely proportional to the square of the distance between the masses, but allows for both attractive and repulsive forces.

In summary, the problem we study in this section is the motion of N charged particles moving on a sphere. Later, in order to produce simulations, we study the specific case of the motion of 3 electrons on the sphere.

6.1 Mathematical Model

We begin with a conducting spherical shell with unit radius. On this sphere we place N charged particles. We denote the mass and charge of the i^{th} particle by m_i and e_i respectively. The configuration manifold is $Q = S^2 \times \cdots \times S^2$ (N times) where the position of a particle is specified by an element of S^2. The Lagrangian for the system is given by

$$L = \frac{1}{2}\dot{q}^T M \dot{q} - V(q)$$

where $q \in S^2$, M is the mass matrix, and $V(q)$ is the potential energy given by

$$V(q) = -\frac{1}{2}\sum_{j\neq i}\frac{e_i e_j}{\|q_j - q_i\|}\,.$$

Notice that we ignore gravitational and magnetic effects.

6.2 Reduction

Due to the spherical symmetry of Q, we see that the Lagrangian is invariant under the action of $SO(3)$. The invariance of L under the action of $SO(3)$ gives rise to the invariance of the angular momentum vector. This calculation can be found explicitly in Section 11.4 of [Marsden, Ratiu]. Briefly, we find that the infinitesimal generator corresponding to $\xi = \hat{\omega} \in \mathfrak{so}(3)$ is

$$\hat{\omega}_P(\mathbf{q}, \mathbf{p}) = (\omega \times \mathbf{q}, \omega \times \mathbf{p})\,.$$

Solving for the momentum map in the standard fashion yields

$$\mathbf{J}(\mathbf{q}, \mathbf{p}) = \mathbf{q} \times \mathbf{p}$$

which is the usual angular momentum vector. Therefore, for the N-body problem on the sphere, we expect all three components of the angular momentum vector to be conserved. The Lagrangian can then be reduced from Q to the quotient space $Q/SO(3)$.

We move now to applying variational integrator techniques to simulate the motion of 3 electrons on the sphere.

6.3 Simulation using a variational integrator

We construct a variational integrator for the 3-electron problem using precisely the same techniques as used in the case of the Astrojax pendulum. The configuration manifold is $Q = S^2 \times S^2 \times S^2$. We embed the configuration manifold in $U = \mathbb{R}^3 \times \mathbb{R}^3 \times \mathbb{R}^3$ so that $Q \subset U$. For coordinates in U, we choose

$$q = \begin{bmatrix} q_1^1 & q_1^2 & q_1^3 & q_2^1 & q_2^2 & q_2^3 & q_3^1 & q_3^2 & q_3^3 \end{bmatrix}^T\,.$$

Notice that $\dim U = 9$. Next, we define the unconstrained Lagrangian $L : U \to \mathbb{R}$ by

$$L = \frac{1}{2}\dot{q}^T M \dot{q} - V(q)$$

where $q \in U$, $M = \mathrm{diag}[m_1, m_1, m_1, m_2, m_2, m_2, m_3, m_3, m_3]$ is the mass matrix, and $V(q)$ is the potential energy given by

$$V(q) = -\frac{1}{2}\sum_{j\neq i}\frac{e_i e_j}{\|q_j - q_i\|}\,.$$

L is the Lagrangian for three electrons free to move in space. Now we define the constrained Lagrangian by restricting L to TQ as follows:

$$L\Big|_{TQ} = L_c : TQ \to \mathbb{R}\,.$$

We impose this restriction by introducing the constraint equation $g : U \to \mathbb{R}^3$ such that $g^{-1}(0) = Q$ where 0 is a regular value of g. Explicitly, we write the constraint equation as

$$g(q) = \begin{bmatrix} (q_1 \cdot q_1) - 1 \\ (q_2 \cdot q_2) - 1 \\ (q_3 \cdot q_3) - 1 \end{bmatrix} = 0\,.$$

Notice that since the constraint is 3-dimensional,

$$\dim Q = 9 - 3 = 6$$

which agrees with our original formulation. To enforce the constraint numerically we introduce the Lagrange multiplier $\mu \in \mathbb{R}^3$. We use the same Discrete Euler-Lagrange Equations as before:

$$\begin{aligned} M\left(\frac{v_{k+1} - 2v_k + v_{k-1}}{h^2}\right) + \frac{1}{2}\left(\frac{\partial V}{\partial q}\left(\frac{v_{k+1} + v_k}{2}\right) \quad + \quad \frac{\partial V}{\partial q}\left(\frac{v_k + v_{k-1}}{2}\right)\right) & \\ -D^T g(v_k)\alpha &= 0 \\ g(v_{k+1}) &= 0 \end{aligned}$$

where

$$\frac{\partial V}{\partial q_k^l} = \sum_{j \neq k} e_j e_k \frac{(q_k^l - q_j^l)}{\|q_k - q_j\|^3}$$

The execution of the algorithm proceeded exactly as for the Astrojax Pendulum only that a Newton-Raphson method was employed involving the iterated solution of a 12-dimensional linear system (9 coordinates and 3 Lagrange multipliers) at each time-step.

The system exhibits interesting dependence on the symmetry of the initial conditions. The initial condition is characterized by the shape of the triangle in the plane formed by the three electrons.

1. The trajectory seen in Figure 3(a) is for an initial condition forming an equilateral triangle on a great circle of the sphere. This configuration is a fixed point of the motion as evidenced by the accompanying movie. Watch Movie.

2. The trajectory in Figure 3(b) is for an initial condition forming an equilateral triangle not on a great circle of the sphere. The symmetry of the initial condition is preserved and the resultant motion is simple "breathing" motion. Watch Movie.

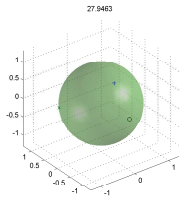

(a) Initial Condition: Equilateral triangle on a great circle.

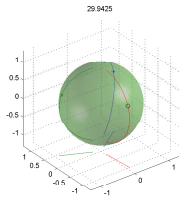

(b) Initial Condition: Equilateral triangle not on a great circle.

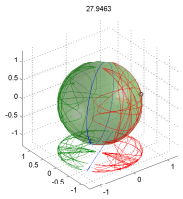

(c) Initial Condition: Isosceles triangle.

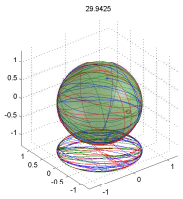

(d) Initial Condition: Scalene triangle.

Figure 3: Trajectories for three electrons on the sphere with various degrees of symmetry in the initial condition.

3. We can break the symmetry of the initial condition above by placing the initial condition in an isosceles triangle formation. Figure 3(c) shows the resulting trajectories. The remaining symmetry is still respected. The red and green trajectories appear chaotic yet exactly mirror one another. The blue trajectory appears to be chaotic also but remains on a great circle. Watch Movie.

4. Finally, we break the symmetry of the initial condition even further by placing the initial condition in a scalene triangle formation. In Figure 3(d), all three particle trajectories appear chaotic on the entire sphere. Watch Movie.

7 Conclusions

We have presented the basic theory in Lagrangian reduction, variational integrators, and pattern evocation. We have applied this theory to two mechanical systems, namely the Astrojax pendulum, and to the motion of three electrons on a conducting sphere. We have demonstrated interesting dynamics and dependence on initial conditions in both cases. Further research will investigate the stability and control of relative equilibria in the Astrojax pendulum as well as the existence and properties of periodic solutions in the N-body problem on the sphere. Generalizations of the N-body problem on the sphere could involve introducing non-Newtonian potentials and more generalized curved manifolds of constraint.

A Euler-Lagrange Equations for the Astrojax Pendulum

λ equation:

$$
\begin{aligned}
0 \;=\;& g m_2 \cos\theta_2 \\
& +2m_2\lambda'\Big((\cos\theta_2\sin\theta_1 - \cos\theta_1\cos(\phi_1-\phi_2)\sin\theta_2)\theta_1' \\
& +(-\cos\theta_2\cos(\phi_1-\phi_2)\sin\theta_1 + \cos\theta_1\sin\theta_2)\theta_2' \\
& +\sin\theta_1\sin\theta_2\sin(\phi_1-\phi_2)(\phi_1'-\phi_2')\Big) \\
& +m_1\lambda'' \\
& +\lambda\Big(-(m_1+m_2-m_2(\cos\theta_1\cos\theta_2+\cos(\phi_1-\phi_2)\sin\theta_1\sin\theta_2))\theta_1'^{\,2} \\
& +m_2(-1+\cos\theta_1\cos\theta_2+\cos(\phi_1-\phi_2)\sin\theta_1\sin\theta_2)\theta_2'^{\,2} \\
& +2m_2\cos\theta_1\sin\theta_2\sin(\phi_1-\phi_2)\theta_1'\phi_1' - m_1\sin\theta_1{}^2\phi_1'^{\,2} - m_2\sin\theta_1^2\phi_1'^{\,2} \\
& +m_2\cos(\phi_1-\phi_2)\sin\theta_1\sin\theta_2\phi_1'^{\,2} - 2m_2\cos\theta_2\sin\theta_1\sin(\phi_1-\phi_2)\theta_2'\phi_2' \\
& +m_2\cos(\phi_1-\phi_2)\sin\theta_1\sin\theta_2\phi_2'^{\,2} - m_2\sin\theta_2{}^2\phi_2'^{\,2} \\
& +m_2\cos\theta_2\sin\theta_1\theta_1'' - m_2\cos\theta_1\cos(\phi_1-\phi_2)\sin\theta_2\theta_1'' \\
& -m_2\cos\theta_2\cos(\phi_1-\phi_2)\sin\theta_1\theta_2'' + m_2\cos\theta_1\sin\theta_2\theta_2'' \\
& +m_2\sin\theta_1\sin\theta_2\sin(\phi_1-\phi_2)\phi_1'' - m_2\sin\theta_1\sin\theta_2\sin(\phi_1-\phi_2)\phi_2''\Big) \\
& +m_2(2\lambda'' + l(\theta_2'^{\,2} + 2\cos\theta_2\sin\theta_1\sin(\phi_1-\phi_2)\theta_2'\phi_2' + \sin\theta_2{}^2\phi_2'^{\,2} \\
& +\sin\theta_1(\cos\theta_2\cos(\phi_1-\phi_2)\theta_2'' + \sin\theta_2\sin(\phi_1-\phi_2)\phi_2''))) - g(m_1+m_2)\cos\theta_1 \\
& -m_2\Big(l(\cos\theta_1\cos\theta_2+\cos(\phi_1-\phi_2)\sin\theta_1\sin\theta_2)\theta_2'^{\,2} + 2\cos\theta_1\cos\theta_2\lambda'' \\
& +\sin\theta_2(\cos(\phi_1-\phi_2)\sin\theta_1(l\phi_2'^{\,2}+2\lambda'') + l\cos\theta_1\theta_2'')\Big)
\end{aligned}
$$

θ_1 Equation:

$$
\begin{aligned}
0 \quad = \quad & \lambda(g(m_1+m_2)\sin\theta_1 + m_2(l-\lambda)(\cos\theta_2\sin\theta_1 - \cos\theta_1\cos(\phi_1-\phi_2)\sin\theta_2){\theta_2'}^2 \\
& -m_1\cos\theta_1\lambda\sin\theta_1{\phi_1'}^2 - m_2\cos\theta_1\lambda\sin\theta_1{\phi_1'}^2 \\
& +2m_2\cos\theta_1\cos\theta_2(l-\lambda)\sin\phi_1 - \phi_2\theta_2'\phi_2' \\
& -lm_2\cos\theta_1\cos(\phi_1-\phi_2)\sin\theta_2{\phi_2'}^2 + m_2\cos\theta_1\cos(\phi_1-\phi_2)\lambda\sin\theta_2{\phi_2'}^2 \\
& -2\lambda'(-(m_1+m_2)\theta_1' + m_2(\cos\theta_1\cos\theta_2\cos(\phi_1-\phi_2) + \sin\theta_1\sin\theta_2)\theta_2' \\
& +m_2\cos\theta_1\sin\theta_2\sin(\phi_1-\phi_2)\phi_2') + m_2\cos\theta_2\sin\theta_1\lambda'' \\
& -m_2\cos\theta_1\cos(\phi_1-\phi_2)\sin\theta_2\lambda'' + m_1\lambda\theta_1'' + m_2\lambda\theta_1'' \\
& +lm_2\cos\theta_1\cos\theta_2\cos(\phi_1-\phi_2)\theta_2'' - m_2\cos\theta_1\cos\theta_2\cos(\phi_1-\phi_2)\lambda\theta_2'' \\
& +lm_2\sin\theta_1\sin\theta_2\theta_2'' - m_2\lambda\sin\theta_1\sin\theta_2\theta_2'' + \\
& -m_2\cos\theta_1(l-\lambda)\sin\theta_2\sin(\phi_1-\phi_2)\phi_2'')
\end{aligned}
$$

ϕ_1 Equation:

$$\begin{aligned}
0 \;=\;& \lambda \sin\theta_1 (m_2(l-\lambda)\sin\theta_2 \sin(\phi_1-\phi_2){\theta_2'}^2 + 2m_1\cos\theta_1 \lambda \theta_1'\phi_1' \\
&+2m_2\cos\theta_1\lambda\theta_1'\phi_1' + 2m_2\cos\theta_2\cos(\phi_1-\phi_2)(l-\lambda)\theta_2'\phi_2' \\
&+lm_2\sin\theta_2\sin(\phi_1-\phi_2){\phi_2'}^2 - m_2\lambda\sin\theta_2\sin(\phi_1-\phi_2){\phi_2'}^2 \\
&+2\lambda'(m_2\cos\theta_2\sin(\phi_1-\phi_2)\theta_2' + (m_1+m_2)\sin\theta_1\phi_1' - m_2\cos(\phi_1-\phi_2)\sin\theta_2\phi_2') \\
&+m_2\sin\theta_2\sin(\phi_1-\phi_2)\lambda'' - lm_2\cos\theta_2\sin(\phi_1-\phi_2)\theta_2'' \\
&+m_2\cos\theta_2\lambda\sin(\phi_1-\phi_2)\theta_2'' + m_1\lambda\sin\theta_1\phi_1'' \\
&+m_2\lambda\sin\theta_1\phi_1'' + m_2\cos(\phi_1-\phi_2)(l-\lambda)\sin\theta_2\phi_2'')
\end{aligned}$$

θ_2 Equation:

$$\begin{aligned}
0 \;=\;& m_2(l-\lambda)(-g\sin\theta_2 + 2\lambda'(-(\cos\theta_1\cos\theta_2\cos(\phi_1-\phi_2)+\sin\theta_1\sin\theta_2)\theta_1' \\
&+\theta_2' + \cos\theta_2\sin\theta_1\sin(\phi_1-\phi_2)\phi_1') + l\cos\theta_2\sin\theta_2{\phi_2'}^2 \\
&-\cos\theta_2\cos(\phi_1-\phi_2)\sin\theta_1\lambda'' + \cos\theta_1\sin\theta_2\lambda'' - l\theta_2'' \\
&+\lambda((\cos\theta_2\cos(\phi_1-\phi_2)\sin\theta_1 - \cos\theta_1\sin\theta_2){\theta_1'}^2 \\
&+2\cos\theta_1\cos\theta_2\sin(\phi_1-\phi_2)\theta_1'\phi_1' + \cos\theta_2\cos(\phi_1-\phi_2)\sin\theta_1{\phi_1'}^2 \\
&-\cos\theta_2\sin\theta_2{\phi_2'}^2 - \cos\theta_1\cos\theta_2\cos(\phi_1-\phi_2)\theta_1'' \\
&-\sin\theta_1\sin\theta_2\theta_1'' + \theta_2'' + \cos\theta_2\sin\theta_1\sin(\phi_1-\phi_2)\phi_1''))
\end{aligned}$$

ϕ_2 equation:

$$\begin{aligned}
0 \;=\;& m_2(l-\lambda)\sin\theta_2(2l\cos\theta_2\theta_2'\phi_2' \\
&+2\lambda'(\cos\theta_1\sin(\phi_1-\phi_2)\theta_1' + \cos(\phi_1-\phi_2)\sin\theta_1\phi_1' - \sin\theta_2\phi_2') \\
&+\sin\theta_1\sin(\phi_1-\phi_2)\lambda'' + l\sin\theta_2\phi_2'' \\
&-\lambda(\sin\theta_1\sin(\phi_1-\phi_2){\theta_1'}^2 - 2\cos\theta_1\cos(\phi_1-\phi_2)\theta_1'\phi_1' \\
&+2\cos\theta_2\theta_2'\phi_2' + \sin(\phi_1-\phi_2)(\sin\theta_1{\phi_1'}^2 - \cos\theta_1\theta_1'') \\
&-\cos(\phi_1-\phi_2)\sin\theta_1\phi_1'' + \sin\theta_2\phi_2''))
\end{aligned}$$

B Variational Integrator for the Astrojax Pendulum

Discrete Euler-Lagrange Equations:

$$\frac{1}{h^2}M\left(q^{k+1}-2q^k+q^{k-1}\right)+\frac{1}{2}\left(\frac{\partial V}{\partial q}\left(\frac{q^{k+1}+q^k}{2}\right)+\frac{\partial V}{\partial q}\left(\frac{q^k+q^{k-1}}{2}\right)\right)-D^Tg(q^k)\mu^{k+1}=0$$

$$g(q^{k+1})=0$$

$$\frac{\partial V}{\partial q}=\begin{bmatrix}0\\0\\m_1g\\0\\0\\m_2g\end{bmatrix}$$

$$\alpha^k:=\frac{1}{\sqrt{(x_1^k)^2+(y_1^k)^2+(z_1^k)^2}}$$

$$\beta^k:=\frac{1}{\sqrt{(x_2^k-x_1^k)^2+(y_2^k-y_1^k)^2+(z_2^k-z_1^k)^2}}$$

$$D^Tg(q^k)=\begin{bmatrix}\alpha^kx_1^k-\beta^k(x_2^k-x_1^k)\\\alpha^ky_1^k-\beta^k(y_2^k-y_1^k)\\\alpha^kz_1^k-\beta^k(z_2^k-z_1^k)\\\beta(x_2^k-x_1^k)\\\beta(y_2^k-y_1^k)\\\beta(z_2^k-z_1^k)\end{bmatrix}$$

$$\begin{bmatrix}m_1(x_1^{k+1}-2x_1^k+x_1^{k-1})\\m_1(y_1^{k+1}-2y_1^k+y_1^{k-1})\\m_1(z_1^{k+1}-2z_1^k+z_1^{k-1})\\m_2(x_2^{k+1}-2x_2^k+x_2^{k-1})\\m_2(y_2^{k+1}-2y_2^k+y_2^{k-1})\\m_2(z_2^{k+1}-2z_2^k+z_2^{k-1})\end{bmatrix}+h^2\begin{bmatrix}0\\0\\m_1g\\0\\0\\m_2g\end{bmatrix}-h^2\mu^{k+1}\begin{bmatrix}\alpha^kx_1^k-\beta^k(x_2^k-x_1^k)\\\alpha^ky_1^k-\beta^k(y_2^k-y_1^k)\\\alpha^kz_1^k-\beta^k(z_2^k-z_1^k)\\\beta(x_2^k-x_1^k)\\\beta(y_2^k-y_1^k)\\\beta(z_2^k-z_1^k)\end{bmatrix}=0$$

$$\frac{1}{\alpha^{k+1}}+\frac{1}{\beta^{k+1}}-l=0$$

So, finally, the Discrete Euler-Lagrange equations are encoded as

$$G(q^{k+1},\mu^{k+1}) = \begin{bmatrix} x_1^{k+1} - 2x_1^k + x_1^{k-1} - h^2 \frac{\mu^{k+1}}{m_1}\left(\alpha^k x_1^k - \beta^k (x_2^k - x_1^k)\right) \\ y_1^{k+1} - 2y_1^k + y_1^{k-1} - h^2 \frac{\mu^{k+1}}{m_1}\left(\alpha^k y_1^k - \beta^k (y_2^k - y_1^k)\right) \\ z_1^{k+1} - 2z_1^k + z_1^{k-1} - h^2 \frac{\mu^{k+1}}{m_1}\left(\alpha^k z_1^k - \beta^k (z_2^k - z_1^k)\right) + h^2 g \\ x_2^{k+1} - 2x_2^k + x_2^{k-1} - h^2 \frac{\mu^{k+1}\beta^k}{m_2}(x_2^k - x_1^k) \\ y_2^{k+1} - 2y_2^k + y_2^{k-1} - h^2 \frac{\mu^{k+1}\beta^k}{m_2}(y_2^k - y_1^k) \\ z_2^{k+1} - 2z_2^k + z_2^{k-1} - h^2 \frac{\mu^{k+1}\beta^k}{m_2}(z_2^k - z_1^k) + h^2 g \\ \frac{1}{\alpha^{k+1}} + \frac{1}{\beta^{k+1}} - l \end{bmatrix} = 0$$

The Jacobian matrix, $J^k \in \mathbb{R}^{7\times 7}$, for this non-linear map is given by

$$J^k := G'(q^k,\mu^k) = \begin{bmatrix} 1 & 0 & 0 \\ 0 & 1 & 0 \\ 0 & 0 & 1 \\ 0 & 0 & 0 \\ 0 & 0 & 0 \\ 0 & 0 & 0 \\ \alpha^k x_1^k - \beta^k (x_2^k - x_1^k) & \alpha^k y_1^k - \beta^k (y_2^k - y_1^k) & \alpha^k z_1^k - \beta^k (z_2^k - z_1^k) \end{bmatrix}$$

$$\begin{bmatrix} 0 & 0 & 0 & -\frac{h^2}{m_1}\left(\alpha^k x_1^k - \beta^k (x_2^k - x_1^k)\right) \\ 0 & 0 & 0 & -\frac{h^2}{m_1}\left(\alpha^k y_1^k - \beta^k (y_2^k - y_1^k)\right) \\ 0 & 0 & 0 & -\frac{h^2}{m_1}\left(\alpha^k z_1^k - \beta^k (z_2^k - x_1^k)\right) \\ 1 & 0 & 0 & -\frac{h^2\beta^k}{m_2}(x_2^k - x_1^k) \\ 0 & 1 & 0 & -\frac{h^2\beta^k}{m_2}(y_2^k - y_1^k) \\ 0 & 0 & 1 & -\frac{h^2\beta^k}{m_2}(z_2^k - z_1^k) \\ \beta^k (x_2^k - x_1^k) & \beta^k (y_2^k - y_1^k) & \beta^k (z_2^k - z_1^k) & 0 \end{bmatrix}$$

Newtons Method gives the update scheme:

$$(q^{k+1},\mu^{k+1}) = (q^k,\mu^k) + \delta^k$$

where δ^k solves the linear system

$$J^k \delta^k = -G(q^k)\,.$$

C Driven Astrojax Pendulum

Physical Constants:

l is the length of the tether.
m_1 mass of bob 1
m_2 mass of bob 2
g is acceleration due to gravity.

Configuration Manifold:

$$\begin{aligned} Q &= \mathbb{R} \times S^2 \times S^2 \\ U &= \mathbb{R}^3 \times \mathbb{R}^3 \\ Q &\subset U \end{aligned}$$

$$\dim U = n = 6$$

Coordinates:

$$q = [x_1\, y_1\, z_1\, x_2\, y_2\, z_2]$$

Lagrangian:

$$L : TU \to \mathbb{R}$$
$$L = \frac{1}{2}\dot{q}^T M \dot{q} - V(q)$$

Mass matrix:

$$M = \begin{bmatrix} m_1 & 0 & 0 & 0 & 0 & 0 \\ 0 & m_1 & 0 & 0 & 0 & 0 \\ 0 & 0 & m_1 & 0 & 0 & 0 \\ 0 & 0 & 0 & m_2 & 0 & 0 \\ 0 & 0 & 0 & 0 & m_2 & 0 \\ 0 & 0 & 0 & 0 & 0 & m_2 \end{bmatrix}$$

Potential:

$$V(q) = g(m_1 z_1 + m_2 z_2)$$

Constrained Lagrangian:

$$L\Big|_{TQ} = L^c : TQ \to \mathbb{R}$$

Driver:

$$A(t) = A_x \mathbf{i} + A_y \mathbf{j} + A_z \mathbf{k}$$

Constraint:

$$g : U \to \mathbb{R} \qquad \text{such that} \qquad g^{-1}(0) = Q$$

where we assume 0 is a regular value of g.

$$g(q) = \sqrt{x_1^2 + y_1^2 + z_1^2 + A_x^2 + A_y^2 + A_z^2 - 2(x_1 A_x + y_1 A_y + z_1 A_z)} + \sqrt{(x_2 - x_1)^2 + (y_2 - y_1)^2 + (z_2 - z_1)^2} - l$$

$$\dim Q = n - 1 = 5$$

Lagrange Multiplier:

$\mu \in \mathbb{R}$ is a Lagrange Multiplier to enforce the constraint.

Discrete Euler-Lagrange Equations:

$$\frac{1}{h^2} M \left(q^{k+1} - 2q^k + q^{k-1}\right) + \frac{1}{2}\left(\frac{\partial V}{\partial q}\left(\frac{q^{k+1}+q^k}{2}\right) + \frac{\partial V}{\partial q}\left(\frac{q^k+q^{k-1}}{2}\right)\right) - D^T g(q^k)\mu^{k+1} = 0$$

$$g(q^{k+1}) = 0$$

$$\frac{\partial V}{\partial q} = \begin{bmatrix} 0 \\ 0 \\ m_1 g \\ 0 \\ 0 \\ m_2 g \end{bmatrix}$$

$$\alpha^k = \frac{1}{\sqrt{(x_1^k)^2 + (y_1^k)^2 + (z_1^k)^2 + (A_x^k)^2 + (A_y^k)^2 + (A_z^k)^2 - 2(x_1^k A_x^k + y_1^k A_y^k + z_1^k A_z^k)}}$$

$$\beta^k = \frac{1}{\sqrt{(x_2^k - x_1^k)^2 + (y_2^k - y_1^k)^2 + (z_2^k - z_1^k)^2}}$$

$$D^T g(q^k) = \begin{bmatrix} \alpha^k(x_1^k - A_x^k) - \beta^k(x_2^k - x_1^k) \\ \alpha^k(y_1^k - A_y^k) - \beta^k(y_2^k - y_1^k) \\ \alpha^k(z_1^k - A_z^k) - \beta^k(z_2^k - z_1^k) \\ \beta(x_2^k - x_1^k) \\ \beta(y_2^k - y_1^k) \\ \beta(z_2^k - z_1^k) \end{bmatrix}$$

$$\begin{bmatrix} m_1(x_1^{k+1} - 2x_1^k + x_1^{k-1}) \\ m_1(y_1^{k+1} - 2y_1^k + y_1^{k-1}) \\ m_1(z_1^{k+1} - 2z_1^k + z_1^{k-1}) \\ m_2(x_2^{k+1} - 2x_2^k + x_2^{k-1}) \\ m_2(y_2^{k+1} - 2y_2^k + y_2^{k-1}) \\ m_2(z_2^{k+1} - 2z_2^k + z_2^{k-1}) \end{bmatrix} + h^2 \begin{bmatrix} 0 \\ 0 \\ m_1 g \\ 0 \\ 0 \\ m_2 g \end{bmatrix} - h^2 \mu^{k+1} \begin{bmatrix} \alpha^k(x_1^k - A_x^k) - \beta^k(x_2^k - x_1^k) \\ \alpha^k(y_1^k - A_y^k) - \beta^k(y_2^k - y_1^k) \\ \alpha^k(z_1^k - A_z^k) - \beta^k(z_2^k - z_1^k) \\ \beta(x_2^k - x_1^k) \\ \beta(y_2^k - y_1^k) \\ \beta(z_2^k - z_1^k) \end{bmatrix} = 0$$

$$\frac{1}{\alpha^{k+1}} + \frac{1}{\beta^{k+1}} - l = 0$$

So, finally, the Discrete Euler-Lagrange equations are encoded as

$$G(q^{k+1},\mu^{k+1}) = \begin{bmatrix} x_1^{k+1} - 2x_1^k + x_1^{k-1} - h^2 \frac{\mu^{k+1}}{m_1}\left(\alpha^k(x_1^k - A_x^k) - \beta^k(x_2^k - x_1^k)\right) \\ y_1^{k+1} - 2y_1^k + y_1^{k-1} - h^2 \frac{\mu^{k+1}}{m_1}\left(\alpha^k(y_1^k - A_y^k) - \beta^k(y_2^k - y_1^k)\right) \\ z_1^{k+1} - 2z_1^k + z_1^{k-1} - h^2 \frac{\mu^{k+1}}{m_1}\left(\alpha^k(z_1^k - A_z^k) - \beta^k(z_2^k - z_1^k)\right) + h^2 g \\ x_2^{k+1} - 2x_2^k + x_2^{k-1} - h^2 \frac{\mu^{k+1}\beta^k}{m_2}(x_2^k - x_1^k) \\ y_2^{k+1} - 2y_2^k + y_2^{k-1} - h^2 \frac{\mu^{k+1}\beta^k}{m_2}(y_2^k - y_1^k) \\ z_2^{k+1} - 2z_2^k + z_2^{k-1} - h^2 \frac{\mu^{k+1}\beta^k}{m_2}(z_2^k - z_1^k) + h^2 g \\ \frac{1}{\alpha^{k+1}} + \frac{1}{\beta^{k+1}} - l \end{bmatrix} = 0$$

The Jacobian matrix, $J^k \in \mathbb{R}^{7\times 7}$, for this non-linear map is given by

$$J^k := G'(q^k,\mu^k) \quad = \quad \begin{bmatrix} 1 & 0 & 0 \\ 0 & 1 & 0 \\ 0 & 0 & 1 \\ 0 & 0 & 0 \\ 0 & 0 & 0 \\ 0 & 0 & 0 \\ \alpha^k(x_1^k - A_x^k) - \beta^k(x_2^k - x_1^k) & \alpha^k(y_1^k - A_y^k) - \beta^k(y_2^k - y_1^k) & \alpha^k(z_1^k - A_z^k) - \beta^k(z_2^k - z_1^k \end{bmatrix}$$

$$\begin{bmatrix} 0 & 0 & 0 & -\frac{h^2}{m_1}\left(\alpha^k(x_1^k - A_x^k) - \beta^k(x_2^k - \right. \\ 0 & 0 & 0 & -\frac{h^2}{m_1}\left(\alpha^k(y_1^k - A_y^k) - \beta^k(y_2^k - \right. \\ 0 & 0 & 0 & -\frac{h^2}{m_1}\left(\alpha^k(z_1^k - A_z^k) - \beta^k(z_2^k - \right. \\ 1 & 0 & 0 & -\frac{h^2\beta^k}{m_2}(x_2^k - x_1^k) \\ 0 & 1 & 0 & -\frac{h^2\beta^k}{m_2}(y_2^k - y_1^k) \\ 0 & 0 & 1 & -\frac{h^2\beta^k}{m_2}(z_2^k - z_1^k) \\ \beta^k(x_2^k - x_1^k) & \beta^k(y_2^k - y_1^k) & \beta^k(z_2^k - z_1^k) & 0 \end{bmatrix}$$

Newtons Method gives the update scheme:

$$(q^{k+1},\mu^{k+1}) = (q^k,\mu^k) + \delta^k$$

where

$$\delta^k = -(J^k)^{-1}\, G(q^k)\,.$$

References

[Wendlandt, Marsden; 1997] Wendlandt, Marsden. 1997. *Mechanical Integrators Derived from a Discrete Variational Principle.*

[Jalnapurkar, Marsden; 1998] Jalnapurkar, Marsden; 1998. *Stabilization of Relative Equilibria*

[Marsden, Scheurle, Wendlandt; 1995] Marsden, Scheurle, Wendlandt. 1995. *Visualization of Orbits and Pattern Evocation for the Double Spherical Pendulum.*

[Marsden, Scheurle; 1994] Marsden, Scheurle; 1994. *Lagrangian Reduction and the Double Spherical Pendulum.*

[Borisov, Mamaev, Kilin; 2004] Marsden, Scheurle; 1994. *Lagrangian Reduction and the Double Spherical Pendulum.*

[Bloch] Bloch; 2003. *Nonholonomic Mechanics and Control.*

[Marsden, Ratiu] Marsden, Ratiu; 1999. *Introduction to Mechanics and Symmetry*